Environmental Processes in the Monterey Bay National Marine Sanctuary: Studies Integrating AVIRIS and Synoptic In Situ Sensing

John Ryan,[1] Francisco Chavez,[1] James Bellingham,[1] Erich Rienecker,[1] Heidi Dierssen[1]
Raphael Kudela,[2] Andrea Vander Woude[2]
Robert Maffione[3]
Andrew Fischer[4]

[1]Monterey Bay Aquarium Research Institute, Moss Landing, California 95039
[2]Department of Marine Sciences, University of California Santa Cruz 95064
[3]Hydro-Optics, Biology, and Instrumentation Laboratories, Tucson, Arizona 85749
[4]Department of Earth and Atmospheric Sciences, Cornell University, Ithaca, New York 14853

Abstract

AVIRIS observations of the Monterey Bay National Marine Sanctuary are presented in light of oceanic processes studied in multidisciplinary field efforts. Field studies in the Monterey Bay region occurred during the second half of August and on October 10-11, 2000. AVIRIS acquisition of the Monterey Bay region was planned to coincide with the field studies. High-altitude AVIRIS overflight on October 13, 2000 spanned near coastal to deep oceanic waters. During the overflight, hyperspectral measurements of downwelling irradiance and upwelling radiance were made at the ocean surface over a large region of the bay. High-resolution *in situ* measurements from an autonomous underwater vehicle during the August field studies revealed complex small-scale processes of significance to coastal ocean ecology. These processes related to upwelling of iron-bearing (fertilizing) sediments, vertical fluxes of carbon at convergent fronts, topographic influences on coastal circulation, and small-scale frontal dynamics. AVIRIS observations captured near-surface structure related to complex small and mesoscale processes, including eddies, filaments, plumes and frontal dynamics, and they defined environmental structure consistent with the *in situ* observations. Application of these advanced sensing methods emphasize the necessity of high spatial and spectral resolution sensing in the dynamic coastal ocean environment and the value of combining remote and *in situ* sensing in studying coastal ocean complexity.

Introduction

The coastal ocean off western North America has received considerable oceanographic study because of its fisheries and proximity to large human populations. The region is strongly influenced by the process of coastal upwelling through which deep waters are drawn to the surface in response to wind-driven transport of surface waters away from the coast. Upwelled waters are nutrient-rich and support high levels of phytoplankton (Figure 1) and higher trophic level production (Ryther, 1969; Barber and Smith, 1981). Dynamic currents of the upwelling system transport upwelled waters and their associated productivity horizontally and vertically by diverse circulation phenomena ranging from the scale of an eastern boundary current to mesoscale eddies and filaments and small-scale frontal dynamics. Off the western United States and Baja California, coastal upwelling occurs seasonally (Bakun et al., 1974; Bakun, 1990). In spring, the Aleutian low pressure system moves northwest and the North Pacific high moves north, resulting in upwelling favorable winds. Equatorward winds continue to force persistent upwelling through spring and early summer; they weaken in late summer and fall and are eventually interrupted by northward winter storm winds, resulting in the cessation of upwelling (Strub et al., 1987a, b).

The Monterey Bay National Marine Sanctuary (MBNMS) lies in the heart of the productive upwelling system off central California (Figure 1). Within this dynamic coastal ocean setting, the Monterey Bay Aquarium Research Institute (MBARI) is developing an Ocean Observing System (MOOS) to advance observational methods and capabilities across the disciplines of geological, chemical, physical and biological oceanography, and spanning research from the ocean surface to the sea floor. MOOS upper-ocean research is founded in sustained observations from moorings and ships that have extended for over a decade (Pennington and Chavez, 2000). These long-term observations provide a framework for understanding local ecosystem function, perturbation by remote forcing such as El Niño (Chavez et al., 2002), and the important ecological questions that may be addressed by advances in methods of remote and *in situ* observation.

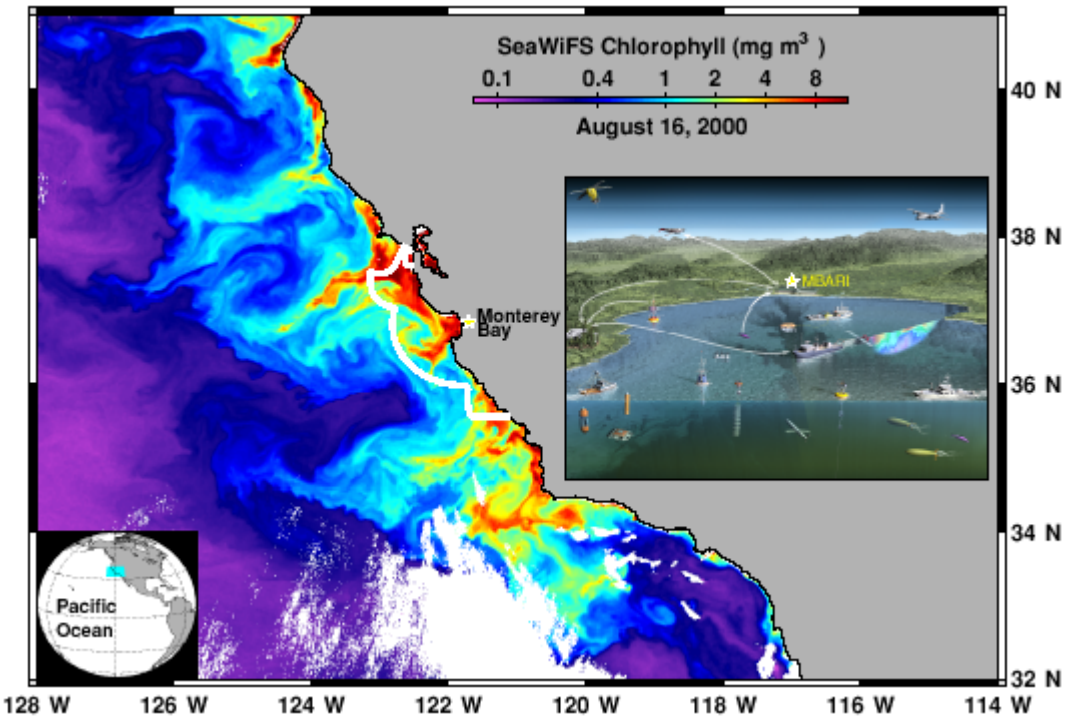

Figure 1. Environmental and experimental context. Main image shows space-based estimates of surface ocean chlorophyll concentrations from SeaWiFS, illustrating the highly productive coastal upwelling system. The white contour overlay defines the boundaries of the MBNMS. Inset image represents activities of the MUSE studies in the Monterey Bay region during August 2000 (see text).

An important approach of MOOS development is to integrate and apply emergent technologies in major field efforts that enable unprecedented ocean sensing while testing the new technologies. During the most recent of these observatory experiments in August 2000, the MOOS Upper-water-column Science Experiment (MUSE; http://www.mbari.org/MUSE), oceanic process studies were focused on the nature and consequences of natural iron fertilization of the coastal food web that occurs through transport of iron-bearing sediments from deep shelf waters into the shallow, sunlit euphotic zone. Iron is a limiting nutrient for phytoplankton, and its importance to oceanic productivity and ecosystem structure in open ocean (Coale et al., 1996; Kudela and Chavez, 1996) and coastal systems (Johnson et al., 1999) is clear. During MUSE participants from 12 research institutions employed a wide array of advanced observing technologies (Figure 1, inset) to pursue diverse science. One of the key technologies was the autonomous underwater vehicle (AUV), an unmanned, untethered robotic submarine programmed to autonomously survey the marine environment (2 yellow submarines at the lower right of Figure 1 inset). Because of their high degree of maneuverability, wide range of flight behaviors, capacity for carrying a multidisciplinary suite of sensors, and relatively rapid propulsion, AUVs are capable of capturing synoptic measurements of the ocean interior that permit greater understanding of complex processes. Most of the *in situ* observations presented here were made using an AUV.

During MUSE there were two primary goals for overflight by the Airborne Visible/Infrared Imaging Spectrometer (AVIRIS; Green et al., 1998). The first was to resolve variability at spatial scales between the high-resolution observations of various moored and mobile *in situ* platforms that cover small regions, and periodic images of satellite ocean color and temperature that cover larger regions at relatively coarse resolution (~1 km). AVIRIS acquisition was intended to fill a scale of observation unachievable by any other means. The second goal was to explore spectral structure of the coastal waters and the science enabled by a highly resolved reflectance spectrum. Having ~2500 times the spatial resolution of a satellite ocean color or infrared image, far greater spectral coverage and resolution than multispectral satellite ocean color sensors, and greatly enhanced signal to noise ratio (Asner and Green, 2001), AVIRIS offers a tremendous opportunity to study near-coastal optical properties, oceanic structure, and processes. Concurrence of AVIRIS and multi-platform *in situ* observation is synergistic.

Methods

The ocean observatory experiment called MUSE occurred as scheduled during the second half of August 2000. AVIRIS acquisition in the Monterey Bay region was planned to coincide with MUSE, however atmospheric conditions precluded high altitude remote sensing of the surface ocean during the experiment (Figure 1 shows conditions immediately before the experiment). Thus a second, shorter research cruise was planned for October 10-11, also intended to coincide with an AVIRIS overflight. The cruise occurred as scheduled on the *R/V Pt. Sur* and included hydro-optical station profiles and continuous underway measurements of temperature, salinity, fluorescence, and spectral absorption and attenuation. The cruise track is shown over regional bathymetry in Figure 2. Conditions during this 2-day cruise were again unsuitable for AVIRIS acquisition. However, on October 13 conditions were favorable, and the overflight occurred. The AVIRIS data spanned near coastal to deep oceanic waters (flight line centers in Figure 2). Coincident with the overflight on October 13, *in situ* hyperspectral measurements of downwelling irradiance and upwelling radiance were made at 18 stations (Figure 2) in a rapid small-boat survey extending into all but the most seaward AVIRIS swath. Additionally, moored hyperspectral and hydrographic measurements were taken within the center flight swath (mooring location in Figure 2). All *in situ* hyperspectral measurements were made with HOBI Labs Hydrorad-4 hyperspectral radiometers.

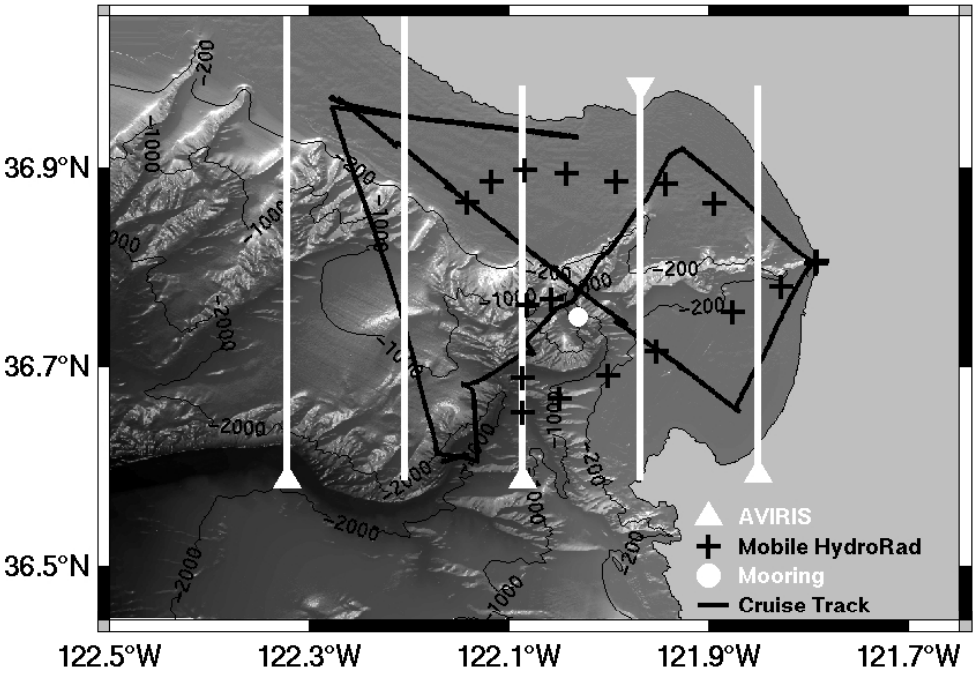

Figure 2. AVIRIS flight lines and ship-based sampling locations shown over bathymetry of the Monterey Bay region (depth contours are 200, 1000, and 2000 m). AVIRIS flight lines and mobile hydrorad stations are from October 13, 2000; cruise track is for the October 10-11 cruise; mooring-based measurements were continuous.

Processing of AUV and ship observations are detailed elsewhere (Ryan et al., in prep). Here we focus on processing of the AVIRIS data. AVIRIS flight line data were obtained from JPL as 512-scanline scenes (Green et al, 1998). The data set consisted of 33 scenes in the five north-south flight lines having ~1 km overlap along their east-west boundaries (Figure 2).

Cross-Track Illumination Correction

Irregularities in cross-track illumination may be due to vignetting effects, instrument scanning, off-nadir view angle and solar reflection, or other non-uniform illumination effects (RSI, 2001b). To avoid sun glint, flight lines for this Monterey Bay region overflight were oriented north-south and intended for acquisition near local noon, which occurred at 12:55 pm on October 13, 2000. AVIRIS acquisition occurred after local noon, between approximately 1:27 and 2:10 pm local time, and some cross-track illumination irregularities were evident in all but

the eastern-most flight line. To reduce cross-track illumination effects in the other four flight lines, we applied a polynomial fit correction method (RSI 2001b).

Atmospheric Correction

Atmospheric correction was accomplished using the Fast Line-of-Sight Atmospheric Analysis of Hyperspectral cubes (FLAASH) atmospheric correction program on each of the flight lines individually. FLAASH is based on the atmospheric physics and spectroscopy of the MODTRAN4 radiative transfer code (Andersen et al., 2000) and models the scattering and absorption processes in the atmosphere with user-supplied parameters. Visibility can be retrieved from the aerosol calculations. However, the assumptions of the aerosol retrieval method (RSI, 2001b), while appropriate for land applications, do not work well over water. We found that this method over-corrected for aerosols and resulted in negative reflectance retrievals. We therefore disabled the aerosol retrieval calculation and specified visibility values using an iterative empirical approach comparing retrieved reflectances with *in situ* surface reflectance measurements made at 18 locations during the AVIRIS overflight. While the scene average visibility calculated by FLAASH was approximately 30 km for all flight lines, the visibility value yielding the closest comparison with *in situ* spectra was 60 km. FLAASH was run in the ISAACS MODTRAN multiple-scattering mode using the atmospheric model of mid-latitude summer and a maritime aerosol profile. In addition to 60 km visibility, we specified a CO_2 mixing ratio of 390 ppm, and an aerosol scale height of 2 km. Corrected flight lines were then joined using pixel-based, overlap-feathering to produce a mosaic image of 3070 x 3914 pixels.

Geometric Correction

An irregular grid of ground control points (GCPs) was constructed from geographic positions provided in the AVIRIS navigation files and supplemented with data from National Ocean Service shoreline data set. GCPs were determined for the center line and edges of each flight line. The flight lines were then transformed into geographic space (latitude and longitude) using the WGS-84 datum and a polynomial warping function in ENVI (RSI 2001a). Nearest-neighbor sampling (Richards and Jia, 1999) was used to assign pixel brightness values.

Other Corrections

The composite image was normalized to account for remaining glint and sea foam effects. For this correction, the reflectance value at 810 nm, a rather flat, low reflectance region of the spectrum, was subtracted from all wavelengths (S. Adler-Golden, communication).

Derived Characteristics of the Marine Environment

Considering the focus of the ocean process studies on phytoplankton ecology, we applied the radiometrically and geometrically corrected AVIRIS oceanic reflectances to derive ocean surface chlorophyll estimates based on algorithms developed for the SeaWiFS satellite sensor (Figure 1). The SeaWiFS OC2 version 4 (OC2V4) modified cubic polynomial and the OC4 version 4 maximum band ratio, 4^{th} order polynomial algorithms were applied (Appendix 1). We present chlorophyll maps from the OC2V4 algorithm. Further algorithm development is underway for suspended sediments, colored dissolved organic matter (CDOM), and characterization of phytoplankton functional groups.

Results

Oceanic Process Studies

In situ observations from the AUV extended over 8 days and provided valuable observations related to upwelling of iron-bearing (fertilizing) sediments, vertical fluxes of carbon at convergent fronts, topographic influences on coastal circulation, and small-scale frontal dynamics resolved in 3-D. Here we present only two examples of AUV observations that illustrate the importance of high-resolution observations.

Physical-Biological Coupling in 3-D

On August 31 2000, an oceanic front was located via underway surface mapping by ship in northern Monterey Bay, and an AUV was deployed to survey a volume around and through the front. Taking nearly 60,000 measurements from each of 6 instruments, the AUV surveyed a volume 7 km x 3 km x 70 meters (Figure 3a). The

gray surface in Figure 3b is a constant density surface (isopycnal) within the volume surveyed, showing a ridge-trough structure in the density field that was aligned with and inshore of the Monterey Canyon shelfbreak. The density ridge coincided with a surface slick that extended as far as the eye could see. The colored contours show mean temperature in the layer 10 to 20 m (11º to 12ºC; 0.2º interval). The coldest waters (dark blue contours) were above the isopycnal ridge. There was a temperature front south of the ridge and small-scale cool/warm eddy-like features south of the front (labeled C and W).

The outer boundary of a concentrated phytoplankton layer is shown as a green isosurface in Figure 3b. Inside this surface, chlorophyll fluorescence was equal to or greater than that along its outer boundary, and fluorescence was much lower everywhere outside this boundary. The highest chlorophyll fluorescence was observed along the southern end of the survey (Chl_{max}), over the trough in the density field. Property distributions are consistent with the concentration of phytoplankton in the trough of an internal wave (Lennert-Cody and Franks, 1999; Pineda, 1999; Franks, 2001). Phytoplankton samples in this region showed high abundance of harmful algal species, thus phytoplankton concentration and patchiness indicated by these observations have implications for transfer of biologically produced toxins through the coastal ocean food web. This complex environmental structure and physical-biological coupling became evident only with a 3-dimensional snapshot of a volume captured from synoptic AUV survey.

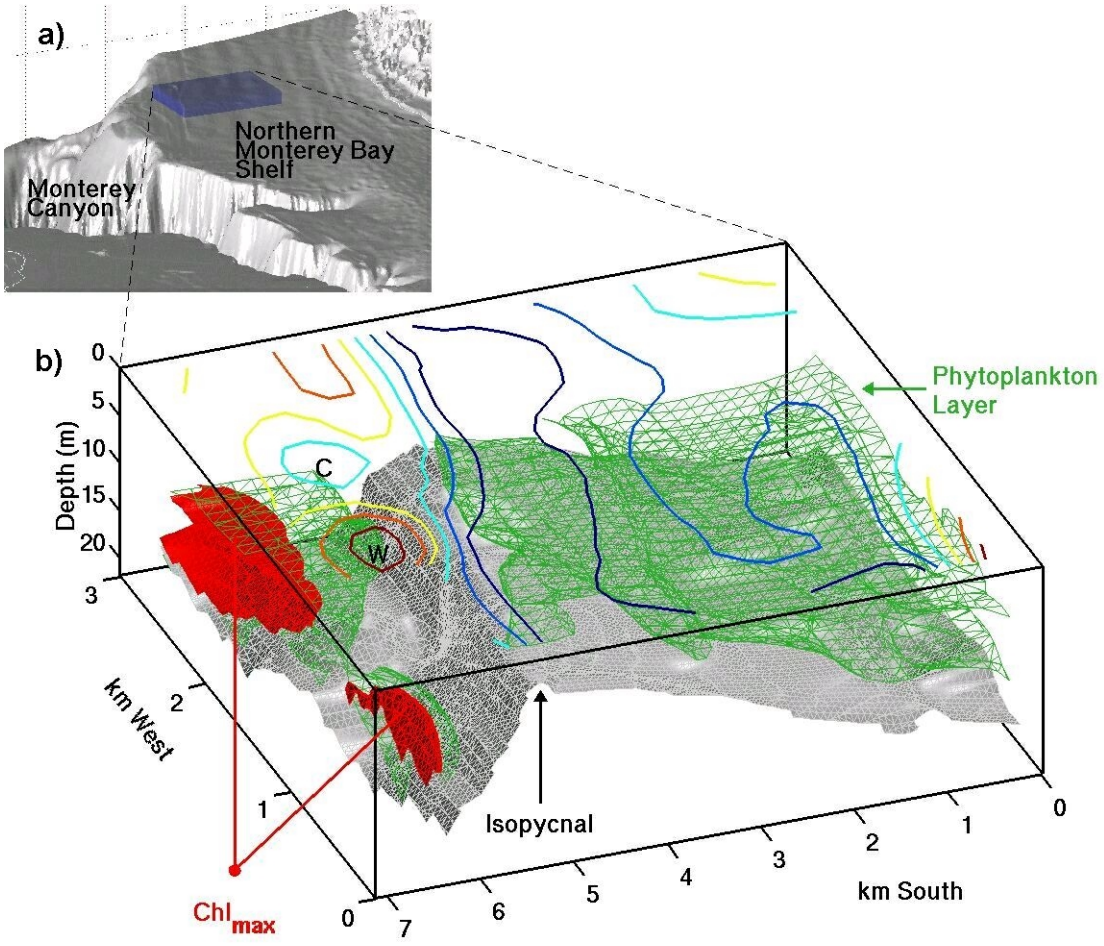

Figure 3. Volume view around a front / density field perturbation on the northern Monterey Bay shelf, 31 August 2000. a) ocean volume (blue) relative to bathymetry (gray); the survey region was near the shelfbreak of Monterey Submarine Canyon. b) observations within volume: the gray isosurface is an isopycnal; the green isosurface is a phytoplankton-rich layer; maximum chlorophyll concentrations are shown in red. The contours are mean temperature between 10 and 20 m (see text).

Exchange between Submarine Canyon and Continental Shelf

Even on scales of a few kilometers, bottom topography can strongly influence ocean circulation on continental shelves; this is an important research area in coastal ocean science (NSF Ocean Sciences Decadal Committee, 2001). Submarine canyons carved into the continental shelf and slope are a ubiquitous feature along the US West Coast (Figure 2). Observational and model studies indicate that cross-shelf exchange and upwelling patterns are profoundly influenced by canyons (Shea and Broenkow, 1982; Freeland and Denman, 1982; Allen 1996; Klinck, 1996; She and Klinck, 2000). AUV-based observations near Monterey Canyon illustrate strong influence of the canyon on regional ecology of benthic and pelagic habitat. During MUSE we mapped physical and bio-optical distributions where a phytoplankton bloom dominated by the diatom *Pseudo-nitzschia australis* was developing. This species produces domoic acid, a neurotoxin harmful to marine life and humans. In 1998, a bloom of *P. australis* resulted in widespread mortality of marine mammals and seabirds (Scholin et al., 2000). On August 30, 2000, in only two hours, we surveyed at high resolution the upper 60-m along an 8-km transect south of Monterey Canyon (Figure 4). This survey allowed examination of the environment and processes surrounding the bloom.

The bloom was concentrated in a subsurface layer approximately 10 m thick. Its vertical distribution closely followed a constant density surface throughout the domain surveyed (Figure 4a,b), indicating close association between the physical environment and the distribution of the phytoplankton. Beneath the bloom was a plume of suspended particulate material emanating from Monterey Canyon (Figure 4c). Particulate material from the bottom can contain iron-bearing sediments that fertilize productivity of the pelagic ecosystem and may contain resting stages of phytoplankton that can initiate blooms when they are transported to shallow, sunlit waters. Iron is thought to be a key regulator of toxin production in *Pseudo-nitzschia* (Maldonado et al., 2002). The lack of toxicity of this bloom may relate to iron supply from canyon upwelling. The patterns observed within the water column, and at the surface (aircraft-mapped SST, not shown) are remarkably consistent with circulation patterns forced by the interaction of flow with the topography of the canyon (Klinck, 1996).

In these case studies, high-resolution, synoptic sensing of the ocean interior with a diverse suite of sensors was essential to understanding processes. We now turn from high-resolution *in situ* sensing to the high spatial and spectral resolution remote sensing from AVIRIS.

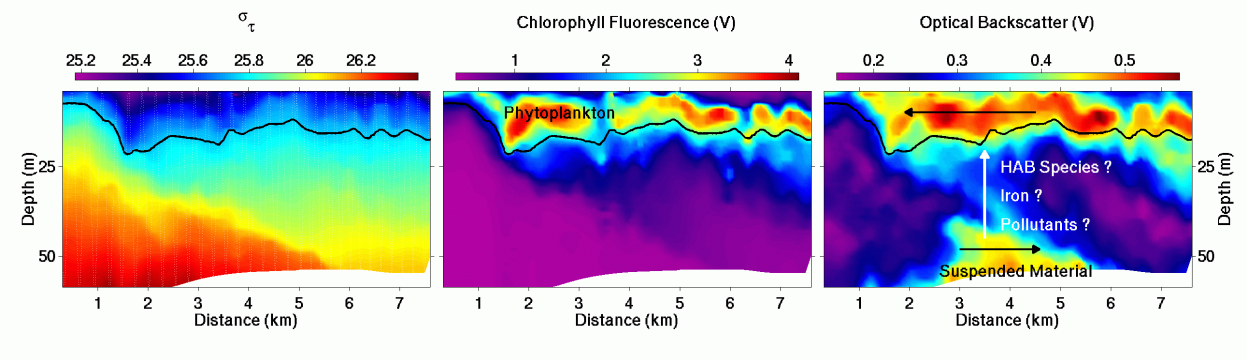

Figure 4. High-resolution vertical sections of 3 of the 6 properties measured using an AUV adjacent to Monterey Canyon on August 30, 2000. The same density level (black contour) is repeated in all panels for reference.

Atmospheric Correction Results

At nearly all *in situ* measurement locations the comparison of ground-truth and image spectra showed good correspondence of spectral shape except in the blue (400-440 nm) region of the spectrum where AVIRIS is less well calibrated (Gao et al., 2000). An example comparison is shown in Figure 5a. At 15 of the 18 stations, comparison of image and *in situ* spectra showed similar characteristics. These are summarized in Figure 5b. The error is characterized as the percent difference between the *in situ* spectra and the spatially-coincident atmospherically corrected image spectrum ([image-*in situ*]/*in situ*). The temporal offset of remote and *in situ* measurements varied between the stations, and this complicates the comparison somewhat; temporal offsets ranged from less than 10 minutes to ~90 minutes. The thick black line in Figure 5b is the median error for the 15 stations. The median error increased from a minimum of ~ 5% at 450 nm to a maximum of ~ 80% toward the IR. We are further examining how atmospheric correction issues (cross-track illumination and glint) affect these comparisons.

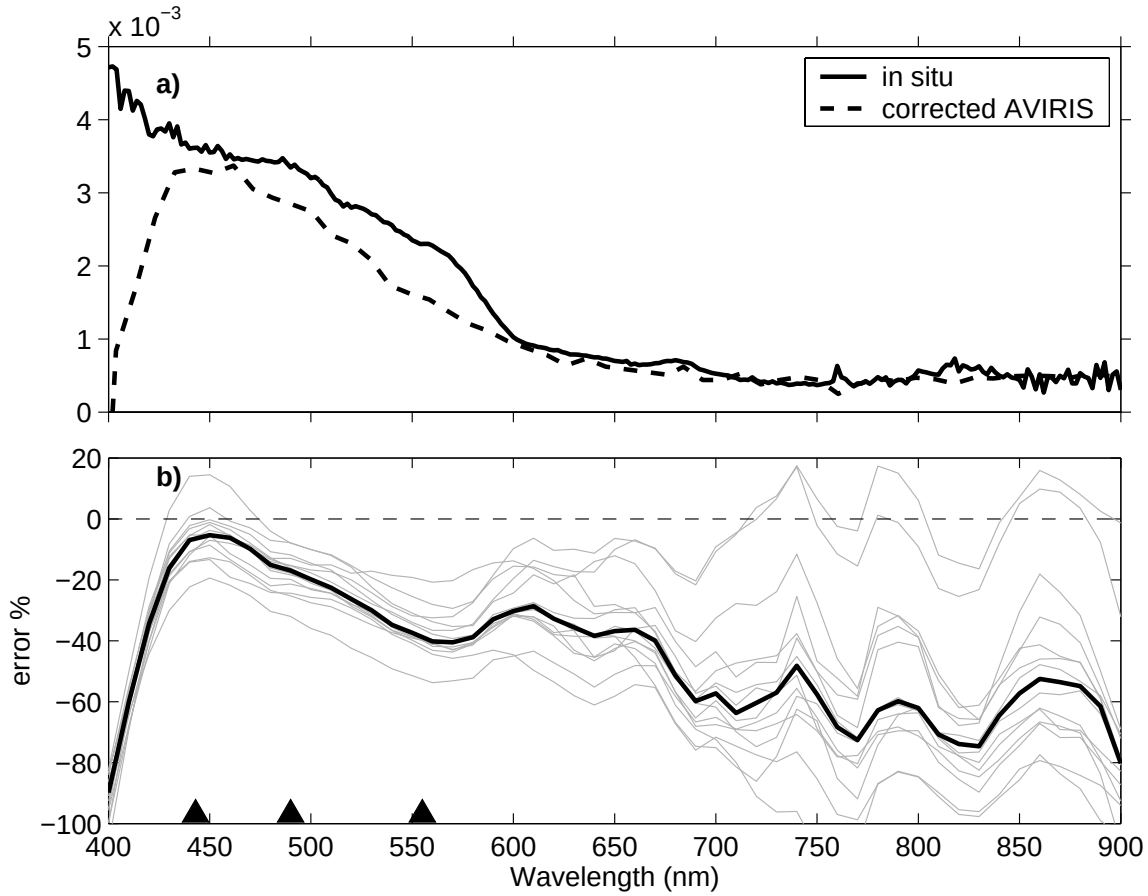

Figure 5. Characterization of error in atmospherically corrected spectra based on ocean surface measurements at 15 locations on the day of AVIRIS overflight. a) example comparison of an *in situ* and AVIRIS corrected spectum, and b) summary for 15 stations; triangles mark wavelengths used for initial chlorophyll estimates (Figure 6).

Surface Chlorophyll Calculated from AVIRIS Data

The surface chlorophyll map derived from the atmospherically corrected reflectance data revealed phenomenal small and mesoscale structure in the Monterey Bay region. A mesoscale hammer-head shaped region of low chlorophyll concentrations extended into the northern and southern shelf waters (Figure 6a). These low chlorophyll plumes were flanked on their seaward sides by relatively high chlorophyll filaments extending from the northern and southern shores toward the bay interior. A high chlorophyll filament extended out of the southern bay into an anticyclonic (clockwise spinning) eddy immediately outside the bay. The highest chlorophyll estimates were in near coastal waters of the northern bay, extending in a plume from the mouth of the Pajaro River. Of course, chlorophyll estimates in this region must be treated carefully as river-borne matter can strongly influence the color of coastal waters.

At the very center of the Monterey Bay crescent is the mouth of Elkhorn Slough (Figure 6b). At this location, the AVIRIS-derived chlorophyll estimates showed a small-scale plume extending from the mouth of the estuary (P label at western boundary of plume). At the core of this plume was a narrow band of high chlorophyll estimates, perhaps indicative of sediments influencing the reflectance and hence calculated chlorophyll. We are currently examining sediment algorithms to study this signature more closely. The highest chlorophyll estimates in this plume region were along the western (seaward) boundary of the plume, consistent with concentration of phytoplankton or other colored organic matter at the outer plume boundary.

Seaward of the Monterey Peninsula (Figure 6c) the map shows a ring of kelp canopy following the topography (labeled k) and fine-scale filaments (labeled F) indicating complex circulation features within the high-chlorophyll filament east of the peninsula. Like the *in situ* observations from the AUV these remotely sensed signatures

emphasize the importance of high spatial resolution in understanding the complex processes of the dynamic coastal ocean.

Spatial Structure from Ship-Based Measurements

Underway surface mapping from the R/V Pt. Sur on October 10 and 11 (ending less than 2 days before the AVIRIS acquisition) revealed surface structure consistent with the AVIRIS chlorophyll map (Figure 7). High chlorophyll fluorescence levels were observed in the region of the northern bay nearshore plume, while low fluorescence and relatively high salinity (relative to the rest of the bay interior) prevailed over the region of the southern bay low-chlorophyll plume evident in the AVIRIS chlorophyll map (Figures 6a,7). The eddy evident in the AVIRIS chlorophyll map (Figure 6a) coincided with warm SST (Figure 7). The warmest, freshest waters surveyed were immediately outside the mouth of Elkhorn Slough (Figure 7), the same plume that showed very complex optical structure (Figure 6b). There are also compelling differences in the region of this plume. While the AVIRIS chlorophyll map suggests relatively low chlorophyll concentrations within the plume (Figure 6b; yellow plume region lower in chlorophyll estimates than the adjacent near-coastal waters), some of the highest chlorophyll fluorescence mapped by the ship were within this plume (Figure 7c). This suggests that either conditions changed between the underway mapping of that region on October 11 and the AVIRIS observations of October 13, or perhaps that absorption in the blue by dissolved substances of estuarine or terrestrial origin affected the chlorophyll estimate based on AVIRIS spectral reflectance.

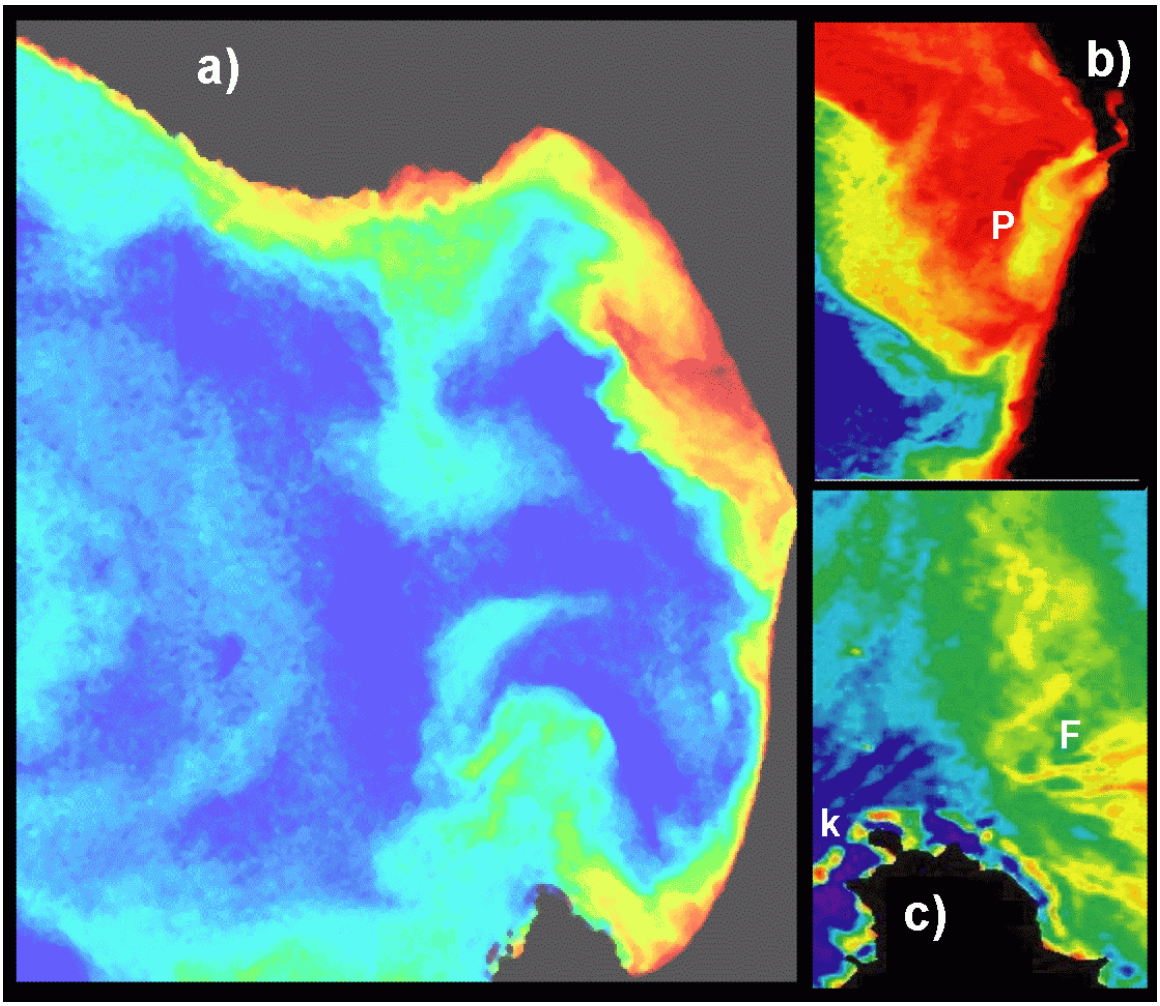

Figure 6. Surface chlorophyll calculated from AVIRIS atmospherically corrected reflectance spectra; ranges differ between the large-area view in a), and the enhanced zoom images around Elkhorn Slough outflow in b) and the Monterey peninsula in c). The range calculated over the entire region was ~0.2 to 8 mg m^{-3}.

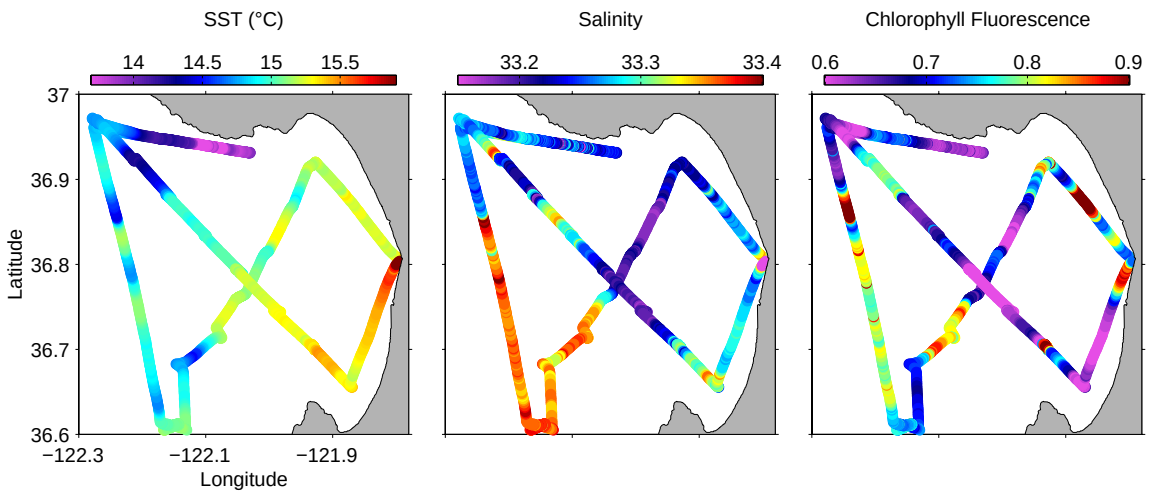

Figure 7. Maps of ocean surface properties measured via the continuous flow system of the R/V Point Sur on October 10-11.

Exploring Spectral Resolution

When and where the color of ocean waters in the upper optical depth is dominated by specific functional groups of phytoplankton, distinct spectral signatures resulting from their unique pigment assemblages may permit mapping of their spatial distributions, as has been shown for Florida Bay (Richardson and Kruse, 1999). We are using a unique time series including moored surface ocean hyperspectral reflectance measurements, moored hydrographic measurements, and regular 3-weekly samples characterizing the pigment and species composition of surface waters at the MBARI M1 mooring in outer Monterey Bay (location shown in Figure 2). Figure 8a shows variability in the shape of the reflectance spectrum over nearly one year at M1 and suggests five periods when the spectrum was markedly different. Changes in the spectrum were clearly related to changes in the underlying ocean structure. For example a sudden change occurred in the spectrum (Figure 8a) as the ocean temperature and salinity fields shoaled in the second period (Figure 8b,c), indicative of the presence of upwelled waters. The third period defined by spectral distinction coincided with hydrographically distinct conditions when surface waters were most persistently cold and saline. There are also indications of relationships between the reflectance spectra and both pigment concentrations and abundance of important phytoplankton groups. For example, chlorophyll was highest during the 3rd and 5th periods of the time series, and the spectral shape during these periods were similar to each other and unique from the other periods. Synechococcus also showed their highest abundance during these periods. Similarly, the 2nd and 4th periods showed similar spectral shapes and were unique compared with the other periods, and they coincided with high abundance of autotrophic flagellates. These patterns are being further examined with a focus on species and functional groups that can dominate the phytoplankton assemblage. Robust relationships from single-location time series will be extended to explore spatial patterns in the spectral gradients of the AVIRIS data relative to the distributions and ecology of important microalgae of this dynamic coastal upwelling environment.

Ongoing and Future Work

Further examination of the AVIRIS atmospheric correction is planned, as described in the results. It is anticipated that improvements to FLAASH specifically for ocean applications (S. Adler-Golden, communication) may improve the atmospheric correction of these data. We are also evaluating the Tafkaa model (Gao et al., 2000) developed by the Naval Research Lab for ocean applications. Motivated by the structure around river and estuarine plumes evident in the AVIRIS-derived chlorophyll maps, we are testing algorithms for sediments and CDOM.

Conclusion

Application of imaging spectroscopy to the coastal ocean is a young science with tremendous promise for delving into the complexity inherent in ocean margin environments so crucial to societal well being. The Monterey Bay region of this dynamic coastal upwelling system, with its history and ongoing development in ocean observing systems, provides a solid basis on which to explore the potential of imaging spectroscopy and its integration with other sensing methods.

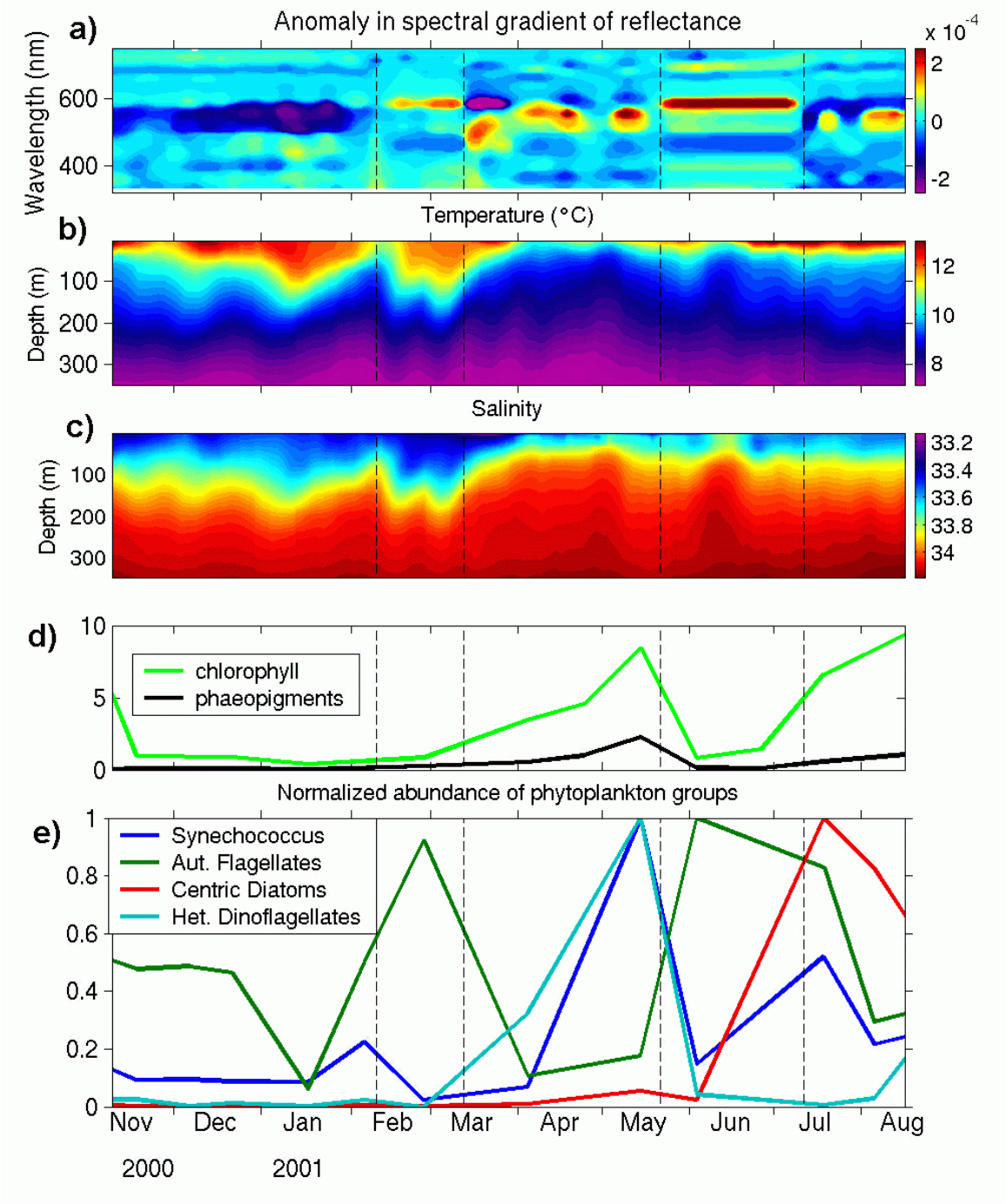

Figure 8. A time series of hyperspectral *in situ* measurements (a) at the mooring location shown in Figure 2 relative to hydrography of the water column (b,c), surface pigments (d) and important local phytoplankton groups (e). The anomaly in the spectral gradient of reflectance (sr^{-1} nm^{-1} x 5) in a) was calculated as follows: A daily reflectance spectrum (calculated from upwelling radiance just below the surface and downwelling irradiance just above the surface) was calculated for the two hour period of each day having the highest downwelling irradiance. To take advantage of the spectral resolution and emphasize variability in spectral shape, the spectral gradient (difference in reflectance / difference in wavelength) was computed. Finally, the anomaly in the spectral gradient was calculated by removing the spectrally resolved temporal mean of the spectral gradient.

Acknowledgments

The observatory research presented was funded by the David and Lucile Packard Foundation. We thank Robert Green (JPL) and Charles McClain (Goddard) for funding the AVIRIS overflight. S. Adler Golden of Spectral Sciences provided invaluable consultation on atmospheric correction. Hydrorad data processing was provided by P. Coenen and E. Palomino.

References

Allen, S.E., 1996. Topographically generated, subinertial flows within a finite length canyon. J. Phys. Oceanogr., 26, 1608-1632.

Andersen, G.P., A. Berk, P.K. Acharya, M.W. Matthew, L.S. Bernstein, J.H. Chetwynd, H. Dothe, S.M. Adler-Golden, A.J. Ratkowski, G.W. Felde, J.A. Gardner, M.L. Hoke, S.C. Richtsmeier, B. Pukall, J. Mello, and L.S. Jeong (2000). MODTRAN4: Radiative transfer modeling for remote sensing, In Algorithms for Multispectral, Hyperspectral, and Ulraspectral Imagery VI, Sylvia S. Chen, Michael R. Descour, Editors, Proceedings of SPIE Vol. 4049, pg. 176-183.

Asner, G. P. and R. O. Green, 2001. Imaging Spectroscopy Measures Desertification in United States and Argentina. EOS 82(49): 601-606.

Bakun, A., 1990. Global climate change and intensification of coastal ocean upwelling. Science 247, 198-201.

Bakun, A., McLain, D.R., Mayo, P.V., 1974. The mean annual cycle of coastal upwelling off western North America as observed from surface measurements. Fish. Bull. 72, 843-844.

Barber, R. T., & Smith, R. L., 1981. Coastal upwelling ecosystems. In Analysis of Marine Ecosystems, (pp. 31-68). New York: Academic Press.

Chavez, F. P., J. T. Pennington, C. G. Castro, J. P. Ryan, R. P. Michisaki, B. Schlining, P. Walz, K. R. Buck, A. McFadyen, and C. A. Collins. 2002. Biological and chemical consequences of the 1997-98 El Niño in central California waters. Progress in Oceanography, 54:205-232.

Coale K. S., K. S. Johnson, S. E. Fitzwater, R. M. Gordon, et al., 1996. A massive phytoplankton bloom induced by an ecosystem-scale iron fertilization experiment in the equatorial Pacifi Ocean. Nature, 383: 495-501.

Franks, P.J.S., 2001. Spatial patterns in dense algal blooms. Limnology and Oceanography, in press.

Freeland, H.J. and K.L. Denman, 1982: A topographically controlled upwelling center off southern Vancouver Island. J. Mar. Res., 40, 1069-1093.

Gao, B-C, M.J. Montes, Z Ahmad, C.O. Davis (2000). Atmospheric correction algorithm for hyperspectral remote sensing of ocean color from space. Applied Optics 39(6) 887-896

Green, R. O. et al., 1998. Imaging Spectroscopy and the Airborne Visible/Infrared Imaging Spectrometer (AVIRIS). Remote Sensing of Environment 65:227-248.

Johnson, K. S., F. P. Chavez, and G. E. Friederich. 1999. Continental-shelf sediment as a primary source of iron for coastal phytoplankton. Nature, 398, 697-700.

Klinck, J.M., 1996: Circulation near submarine canyons: A modeling study. J. Geophys. Res., 101, 1211-1223.

Kudela, R. M. and F. P. Chavez, 1996. Bio-optical properties in relation to an algal bloom caused by iron enrichment in the equatorial Pacific. Geophysical Research Letters, 23(25):3751-3754.

Lennert-Coty, C. E. and P. S. J. Franks, 1999. Plankton patchiness in high-frequency internal waves. Marine Ecology Progress Series, 186: 59-66.

Maldonado, M. T., M. P. Hughes, E. L. Rue, and M. R. Wells, 2002. The effect of Fe and Cu on growth of domoic acid production by Pseudo-nitzschia multiseries and Pseudo-nitzschia australis. Limnol. Oceanogr. 47(2):515-526.

NSF Ocean Sciences Decadal Committee, 2001, Ocean Sciences at the New Millennium, 152 pp.

Pennington, J. T. and F. P. Chavez, 2000. Seasonal fluctuations of temperature, salinity, nitrate, chlorophyll, and primary production at station H3/M1 over 1989-1996 in Monterey Bay, California. Deep-Sea Research, Part II, 47:947-973.

Pineda, J., 1999. Circulation and larval distribution in internal tidal bore warm fronts. Limnology and Oceanography 44(6):, 1400-1414.

Richards, J.A and X. Jia, 1999. Remote Sensing Digital Image Analysis: An Introduction. 3rd Edition. Springer.

Richardson, L. L. and F. A. Kruse, 1999. Identification and classification of mixed phytoplankton assemblages using AVIRIS image-derived spectra. Summaries of the Eighth JPL Airborne Earth Science Workshop, Pasadena, CA, JPL Publication 99-17.

RSI, 2001a, ENVI User's Guide. September 2001 edition. Research Systems.

RSI,2001b, FLAASH User's Guide. Version 1.0. Research Systems.

Ryan, J., F. Chavez, J. Bellingham, C. Scholin, J. Bellingham, J. Paduan, S. Ramp. Phytoplankton layers and related processes in Monterey Bay, California, in prep.

Ryther, J. H., 1969. Photosynthesis and fish production in the sea. *Science* **166**: 72-76.

Scholin, C. A. et al., 2000. Mortality of sea lions along the central California coast linked to a toxic diatom bloom. Nature, 403:80-84.

She, J. and J.M. Klinck, 2000: Flow near submarine canyons driven by constant winds. J. Geophys. Res., 105, 28,671-28,694.

Shea, R. E. and W. W. Broenkow, 1982. The role of internal tides in the nutrient enrichment of Monterey Bay, California. Estuarine, Coastal and Shelf Science, 15:57-66.

Strub, P.T., Allen, J.S., Huyer, A., Smith, R.L., 1987a. Large-scale structure of the spring transition in the coastal ocean off western North America. Journal of Geophysical Research 92, 1527-1544.

Strub, P.T., Allen, J.S., Huyer, A., Smith, R.L., Beardsely, R.C., 1987b. Seasonal cycles of currents, temperatures, winds, and sea level over the northeast Pacific continental shelf. Journal of Geophysical Research 92, 1507-1527.

Appendix 1.

Chlorophyll algorithms used for corrected AVIRIS reflectances.

***Table 1*: Version 4 of SeaWiFS chlorophyll algorithms OC4 and OC2 used for initial chlorophyll estimates from corrected AVIRIS data.**

Coefficients for OC4 version 4 (Maximum Band Ratio, 4th Order Polynomial)

a = [0.366,-3.067,1.930,0.649,-1.532]
R = ALOG10((Rrs443>Rrs490>Rrs510)/Rrs555)
Chl a (ug/l) = 10.0^(a(0) + a(1)*R + a(2)*R^2 + a(3)*R^3 + a(4)*R^4)

Coefficients for OC2 version 4 (Modified Cubic Polynomial)

a = [0.319, -2.336, 0.879, -0.135, -0.071]
R = ALOG10(Rrs490/Rrs555)
Chl a (ug/l) = 10.0^(a(0) + a(1)*R + a(2)*R^2 + a(4)

http://seawifs.gsfc.nasa.gov/SEAWIFS/RECAL/Repro3/OC4_reprocess.html